DOI: 10.13009/EUCASS2023-853
Aerospace Europe Conference 2023 – 10TH EUCASS – 9TH CEAS

Region of Attraction Estimation Using Multiple Shape Functions in Sum-of-Squares Optimization for Aircraft Flight Control System

Bhaskar Biswas[⋆], *Dmitry Ignatyev*[†], *Argyrios Zolotas*[‡] & *Antonios Tsourdos*[§]
School of Aerospace, Transport and Manufacturing, Cranfield University
Bedford MK43 0AL, UK
[⋆]bhaskar.biswas@cranfield.ac.uk, [†]D.Ignatyev@cranfield.ac.uk
[†]A.Zolotas@cranfield.ac.uk & [§]a.tsourdos@cranfield.ac.uk

Abstract
Flight control clearance and flight envelope certification are vital steps for guaranteeing flight safety. While there exist numerical techniques for flight dynamics analysis, these tend to be limited in their predictive capabilities given their dependence to either linearized system dynamics or their conservativeness. This paper proposes a new method contributing to the roadmap toward flight certification that expands the safe flight envelope by incorporating multiple Shape Functions within the sum-of-squares optimization framework. The technique, formulated using polynomial Lyapunov functions, ensures controller stability and performance. The proposed approach achieves a larger region of attraction estimation. The method is validated via the estimation of a region of attraction for closed-loop polynomial dynamics of the Vought F-8 Crusader aircraft. The effectiveness of the method is demonstrated through extensive simulations, illustrating its applicability in flight control system analysis and providing an expanded safe, and stable operating region. The enhanced region of attraction offers improved operational flexibility, as well as safety margins and system performance.

1. Introduction

The utilization of advanced control techniques in aerospace systems has gained significant attention due to their potential to enhance safety, efficiency, and overall performance. Closed-loop systems, which integrate feedback control mechanisms, are particularly prevalent in aircraft dynamics, enabling precise manoeuvring, stability, and response characteristics. A fundamental aspect of closed-loop systems is the determination of the region of attraction (ROA), which defines the set of initial states where the system is guaranteed to converge to a stable equilibrium point, Khalil.[1] The presence of a ROA in a closed-loop system paves the way for validating the designed controller. Enlarging the ROA is of paramount importance as it allows for greater operational flexibility, improved safety margins, and enhanced system performance. The estimation of the ROA for complex nonlinear dynamical systems is a challenging task, often requiring sophisticated mathematical and computational methods.

One effective approach to estimating the region of attraction (ROA) is through the utilization of sum-of-squares (SOS) optimization method. SOS optimization enables the estimation of the ROA for the closed-loop system, providing guarantees on the stability and performance of the controller by formulating a polynomial Lyapunov function (LF). In this article, we demonstrate the advantages of the SOS optimization technique in estimating an enhanced ROA for a polynomial closed-loop system of the Vought F-8 Crusade aircraft, which validates and provides a safe operating area for the controller.

SOS optimization method is based on the SOS polynomial. An SOS polynomial is characterized as a non-negative polynomial expressed as the sum of squares of other polynomials. Due to the non-negativity of both Lyapunov functions (LFs) and SOS polynomials, an LF can be represented as an SOS polynomial. The SOS methodology expands the applicability of linear matrix inequality (LMI) techniques. A comprehensive understanding of LMIs and their use for approximating the region of attraction (ROA) can be found in VanAntwerp[2] and Tibken.[3] In Powers,[4] the authors present an algorithm that determines whether a real polynomial is an SOS polynomial and discovers its representation if applicable. As a relaxation technique, SOS investigates the necessary conditions for expressing a non-negative

DOI: 10.13009/EUCASS2023-853

polynomial as a relaxed SOS polynomial, as discussed in Parrilo[5] and Parrilo.[6] Resources providing instruction on the SOS optimization method, including MATLAB code for calculating the ROA, are available in Balas,[7] Peet,[8] and Papachristodoulou.[9] In Cunis,[10] the authors propose an algorithm that effectively addresses nonconvex SOS problems. Software tools such as SOSOPT [Seiler[11]], BiSOS [Cunis[10]], and SOSTOOLS [Papachristodoulou[12]] are specifically designed to handle challenges related to SOS optimization. For further details on the SOS optimization technique, interested readers can refer to Ahmadi,[13] Lall,[14] and Kunisky.[15]

The application of the SOS optimization technique for controller design and ROA estimation is demonstrated in the works of Wloszek,[16] Tan,[17] Jarvis-Wloszek,[18] and Tan.[19] In Chakraborty,[20] Khrabrov,[21] and Li,[22] the authors utilized the SOS optimization method to estimate the ROA for aircraft attractors. These studies incorporated a Shape Function (SF) approach to obtain a larger ROA. However, if the actual ROA is non-symmetric, the method still yields conservative results. In order to overcome these constraints, Biswas[23] introduced the Union Theorem as a solution to estimate the ROA for polynomial dynamical systems with non-symmetric or constrained actual ROA. The Union Theorem enables the utilization of multiple SFs to obtain an enhanced ROA.

The objective of this paper is to employ the Union Theorem within the SOS optimization framework to estimate an enhanced ROA for the complex closed-loop polynomial dynamics of the Vought F-8 Crusader aircraft, specifically focusing on its short-period mode. By leveraging the Union Theorem, it becomes possible to incorporate multiple SFs within the SOS optimization framework, resulting in an enhanced ROA estimation. This estimation aims to validate the controller and identify an improved safe operating region for the aircraft.

This paper is organized as follows: Section 2 presents the aircraft's polynomial dynamics, background on SOS optimization, and problem formulation. Section 3 explains the method to estimate the enhanced ROA, utilizing the Union Theorem within the SOS optimization framework. In Section 4, the numerical resolution process is detailed. Section 5 describes the selection process of the necessary SF. Simulation outcomes are showcased in Section 6. Finally, Section 7 offers concluding remarks.

2. Preliminaries and Problem Formulation

2.1 The Vought F-8 Crusader Aircraft Polynomial Dynamics Model

For this study, the selected nonlinear polynomial aircraft model focuses on the nominal closed-loop short-period dynamics of the Vought F-8 Crusader aircraft as referenced in Zhao.[24] Disregarding drag, the essential nonlinear equations that illustrate the closed-loop short-period mode are,

$$\dot{\alpha} = -0.878\alpha + q - \alpha^2 q - 0.0896\alpha q - 0.019\theta^2 + 0.473\alpha^2 + 3.813\alpha^3 - 0.216\delta_e \tag{1a}$$

$$\dot{\theta} = q \tag{1b}$$

$$\dot{q} = -4.209\alpha - 0.396q - 0.408\alpha^2 - 2.137\alpha^3 - 20.991\delta_e \tag{1c}$$

$$\begin{aligned} \text{where, } \delta_e = &-0.60357\alpha + 0.51918\theta + 2.6414q + 1.1853\alpha^2 - 0.0039012\theta^2 + 0.15242q^2 - 0.2542\alpha\theta - 0.58084\alpha q \\ &+ 0.15914\theta q + 8.0966\alpha^3 + 0.077795\theta^3 + 0.25808q^3 - 1.9417\alpha^2\theta - 4.2947\alpha^2 q + 0.5879\alpha\theta^2 + 0.34048\alpha q^2 \\ &+ 0.077199\theta^2 q - 0.13242\theta q^2 + 0.69357\alpha\theta q \end{aligned} \tag{1d}$$

Let us consider,

$$\dot{x} = \begin{bmatrix} \dot{\alpha} \\ \dot{\theta} \\ q \end{bmatrix}; \quad f_0(x) = \begin{bmatrix} -0.878\alpha + q - \alpha^2 q - 0.0896\alpha q - 0.019\theta^2 + 0.473\alpha^2 + 3.813\alpha^3 \\ q \\ -4.209\alpha - 0.396q - 0.408\alpha^2 - 2.137\alpha^3 \end{bmatrix}; \quad g_0(x) = \begin{bmatrix} -0.216 \\ 0 \\ -20.991 \end{bmatrix} \tag{2}$$

The Eq. (1) can be represented as below,

$$\dot{x} = f_0(x) + g_0(x)u = f(x), \quad \text{where, } u = \delta_e \text{ (Elevator Deflection)} \tag{3}$$

Here, the trim point x = 0 is an equilibrium point (EP). The objective is to estimate an enhanced ROA of this closed-loop system such that the angle of attack (α), pitch angle (θ), and pitch rate (q) come to the EP within a large range of disturbances.

DOI: 10.13009/EUCASS2023-853

2.2 SOS Optimization

Some important definitions related to SOS optimization,Wloszek,[16]

Definition 1 (Positive Semi-definite Polynomial) *A polynomial, $f(x)$, is called Positive Semi-definite Polynomial if $f(x) \geq 0$ for all $x \in \mathbb{R}^n$*

Definition 2 (Sum-of-Squares (SOS) polynomial) *A polynomial, $s(x) \in \mathcal{R}_n$ is a SOS polynomial if there exist polynomials $f(x)_i \in \mathcal{R}_n$ such that*

$$s(x) = \sum_{i=1}^{t} f_i^2,\ f_i \in \mathcal{R}_n, i = 1, ..., t$$

Again, s(x) is an SOS if there exists $Q \geq 0$ such that $s(x) = Z^T QZ$, where Z is the vector of monomials. The set of SOS polynomials in n variables is defined as

$$\sum\nolimits_n := \left\{ s(x) \in \mathcal{R}_n \,\middle|\, s(x) = \sum_{i=1}^{t} f_i^2,\ f_i \in \mathcal{R}_n, i = 1, ..., t \right\}$$

Now, always $s(x) \geq 0$ if $s(x) \in \sum_n \ \forall\ x \in \mathbb{R}^n$.

Definition 3 (Region of Attraction) *Let us consider $\phi(x)$ as the solution of the system expressed by Eq. (3). The ROA of origin, $x = 0$ (EP) is, Khalil,[1]*

$$R_A = \{x \in \mathbb{R}^n : \phi(x) \ is\ \forall\ t \geq 0\ and \lim_{t\to\infty} \phi(x) \to 0\}$$

Lemma 1 *Let us consider that $\dot{x}$ represents the closed-loop dynamics of the system. If there exist a continuously scalar function $V(x) : \mathbb{R}^n \to \mathbb{R}$ and a positive scalar $\gamma \in \mathbb{R}^+$, such that,*

$$V(x) > 0\ \forall\ x \neq 0\ and\ V(0) = 0 \tag{4a}$$

$$\Omega_\gamma = \{x : V(x) \leq \gamma\}\ is\ bounded \tag{4b}$$

$$\Omega_\gamma \subseteq \{x : \frac{\partial V}{\partial x}\dot{x} < 0\} \cup \{0\} \tag{4c}$$

Then the origin is asymptotically stable and $\Omega_\gamma \subseteq R_A$, Vidyasagar.[25]

If the value of γ is unbounded, it implies that the system is globally asymptotically stable. The mentioned lemma establishes a bounded LF, denoted as $V(x)$, by constraining the value of γ. By optimizing the level of γ, the largest possible estimation of Ω_γ can be obtained. The SOS optimization method is one approach that can be used to optimize γ. This method allows for the simultaneous determination of the Lyapunov function, $V(x)$, which is expressed as a sum-of-squares function, and the optimized value of γ.

2.2.1 SOS Optimization form of the ROA

The objective is to expand the ROA, denoted as Ω_γ, for the system described by Equation (3). The approach for estimating the maximized ROA can be formulated within the following SOS optimization framework, [Biswas,[23] Wloszek[16]],

$$\gamma^* = \max_{\mathbf{s_0} \in \sum_\mathbf{n}} \gamma$$

$$\text{Subject to}:\ V(x) - l_1 \in \sum\nolimits_n \tag{5a}$$

$$-\Big[\frac{\partial V}{\partial x} f(x) + l_2\Big] + (V(x) - \gamma)s_0 \in \sum\nolimits_n \tag{5b}$$

Here, l_1 and l_2 are SOS polynomials. The above equation estimates a very small ROA, as discussed and demonstrated in Biswas.[23] To improve the ROA estimation, a new function called shape function (SF) has been introduced in Wloszek[16] along with Eq. (5), and we will discuss this further in the next section.

DOI: 10.13009/EUCASS2023-853

2.2.2 Shape Function

The Shape function (SF) represents a function with an enclosed region that is circumscribed by the bounded LF. It prompts the bounded LF to grow by enlarging the size of the SF itself in each iteration until a portion of the LF makes contact with the unstable region. In other words, the SF establishes the concluding form and scale of the bounded LF. The integration of the SF into the SOS optimization method can be achieved in the following manner, [Biswas,[23] Wloszek[16]],

Definition 4 (Shape Function) *SF is a positive definite function. The variable size region under it is defined as,*

$$P_\beta := \{x : p(x) \leq \beta\} \subseteq \Omega_\gamma \tag{6}$$

If we introduce the SF in the Eq. (5) then we get the following modified optimization form of Eq. (5),

$$\beta^* = \max_{\mathbf{s_0},\, \mathbf{s_1} \in \sum_\mathbf{n},\; V(x) \in \mathcal{R}_n,\; \gamma \in \mathbb{R}^+} \beta$$

$$\text{Subject to}: V(x) - l_1 \in \sum\nolimits_n \tag{7a}$$

$$-\Big[\frac{\partial V}{\partial x} f(x) + l_2\Big] + (V(x) - \gamma)s_0 \in \sum\nolimits_n \tag{7b}$$

$$-(V(x) - \gamma) + (p(x) - \beta)s_1 \in \sum\nolimits_n \tag{7c}$$

Eq. (7) illustrates the process of maximizing the variable β, which in turn leads to the determination of optimal values for both V and γ. It should be noted that the introduction of an SF does not modify the existing equation expressed by Eq. (5), but rather imposes an additional constraint. The incorporation of a single SF alongside Eq. (5) yields superior outcomes compared to utilizing Eq. (5) alone. However, it is important to recognize that Eq. (7) only estimates a portion of the actual ROA, particularly for systems with non-symmetric or unbounded actual ROA. This topic is thoroughly discussed and demonstrated in Biswas.[23] To address this concern, the Union Theorem is proposed by Biswas,[23] and its details are discussed in the subsequent section.

3. Enhanced ROA Estimation Using Multiple Shape Functions

Eq. (7c) indicates that the region enclosed by the SF must be limited within the boundaries defined by the LF and its associated γ value. An SOS optimization tool, such as SOSOPT, gradually increases the parameter β in each iteration, allowing more regions to fall under the SF. Consequently, a new LF is generated, ensuring full coverage of the SF's area while maintaining a constant γ. This iterative process, known as the V-S iteration, will be discussed in detail in a subsequent section.

In order to estimate the ROA using a single SF in SOS optimization, as described by Eq. (7), the V-S iteration algorithm is employed to expand the estimation of the ROA through an increased number of iterations. However, this approach is not universally applicable. For instance, in cases of early convergence during optimization and/or numerical infeasibility, especially for systems with unbounded or irregular ROA, this method may prove ineffective. Additionally, the limitation of the estimation arises from the fixed or adaptive placement of the geometric center of the SF at the origin, particularly when dealing with non-symmetric or unbounded ROA. The issue is that after a certain number of iterations, the SF may approach the boundary of a non-symmetric ROA in a particular direction. Subsequent increments of β may not yield new LF that fully enclose the region under the SF, as the SF is on the verge of touching the boundary in that particular direction. While the estimated ROA may closely align with the true ROA in certain regions of the boundary, it ceases to expand in other regions. To address this issue, Union Theorem has been proposed in Biswas.[23]

Theorem 1 (Union Theorem) *Let us consider the given polynomials V, p_1, p_2,...,p_n define sets A_V, A_1, A_2,...,A_n such that,*

$$\begin{aligned} A_V &= \{x \in \mathbb{R}^n : V - \gamma \leq 0\} \\ A_1 &= \{x^1 \in \mathbb{R}^n : p_1 - \beta_1 \leq 0\} \\ A_2 &= \{x^2 \in \mathbb{R}^n : p_2 - \beta_2 \leq 0\} \\ &\vdots \\ A_n &= \{x^n \in \mathbb{R}^n : p_n - \beta_n \leq 0\} \end{aligned}$$

DOI: 10.13009/EUCASS2023-853

Here, $\{\gamma, \beta_1, \beta_2, ..\beta_n\} \in \mathbb{R}^+$. *Now if there exit polynomials* $s_1 \in \sum_n$, $s_2 \in \sum_n, ..., s_n \in \sum_n$, *such that,*

$$-(V-\gamma)+(p_1-\beta_1)s_1 \in \sum\nolimits_n$$
$$-(V-\gamma)+(p_2-\beta_2)s_2 \in \sum\nolimits_n$$
$$\vdots$$
$$-(V-\gamma)+(p_n-\beta_n)s_n \in \sum\nolimits_n$$

Then, $A_1 \cup A_2 \cup ... \cup A_n \subseteq A_V$.

The Union Theorem tells us that if we introduce multiple SFs ($p_{1,..,n}$) in different places then we can get an LF (V), which will encircle all of them. If we incorporate the Union Theorem with the Eq. (7), then the modified form of the Eq. (7) can be expressed in the following way,

$$[\beta_1^*, \beta_2^*, ..., \beta_n^*] = \max_{\mathbf{s_0,s_1,s_2,...,s_n} \in \sum_\mathbf{n},\ ,V(x)\in\mathcal{R}_n,\ \gamma\in\mathbb{R}^+} \beta_1, \beta_2, ..., \beta_n$$

$$\text{Subject to:} \quad V - l_1 \in \sum\nolimits_n \tag{8a}$$

$$-\left[\frac{\partial V}{\partial x} f(x) + l_2\right] + (V-\gamma)s_0 \in \sum\nolimits_n \tag{8b}$$

$$-(V-\gamma)+(p_1-\beta)s_1 \in \sum\nolimits_n \tag{8c}$$

$$-(V-\gamma)+(p_2-\beta_2)s_2 \in \sum\nolimits_n \tag{8d}$$

$$\vdots$$

$$-(V-\gamma)+(p_n-\beta_n)s_n \in \sum\nolimits_n \tag{8n}$$

Remark 1. Eq. (8a) ensures the positive definiteness of V, which is the 1st condition for a LF.

Remark 2. Eq. (8b) tells us that the region enclosed by $V \leq \gamma$ should be always inside the stable region as $\dot{V} \leq -l_2$.

Remark 3. Eq. (8c)-(8n) make sure that the regions enclosed by $p_1 \leq \beta_1, ..., p_n \leq \beta_1$ should be always inside the region enclosed by $V \leq \gamma$.

The V-S iteration algorithm is applied to resolve Eq. (8). With each iteration, the algorithm elevates the value of all β for every SF, leading to an accompanying LF, which encompasses additional regions by encircling all of the SFs. Although the algorithm employing multiple SFs might cease if a specific SF comes into contact with the unstable area in one direction, by then it has already produced an expanded ROA. This growth results from the increase of all SFs in various directions, thereby broadening the ROA in multiple ways.

4. Numerical Algorithm

The $V-s$ iteration algorithm solves Eq. (8) by employing three steps, namely the γ-step β-step, and V-step, [Biswas,[23] Wloszek[16]]. The first two steps named γ-step, β-step involve optimizing γ and β_i, respectively, while the third step named V-step is a feasibility problem that finds a new LF V that satisfies all constraints under it. The algorithm is outlined as follows,

V-s Iteration Algorithm:

1. γ**-step:** Solve for s_0 and γ^* for a given V and fixed l_2 :

$$\gamma^* = \max_{\mathbf{s_0}\in\sum_n} \gamma \quad \text{s.t.}: -\left[\frac{\partial V}{\partial x} f(x) + l_2\right] + (V-\gamma)s_0 \in \sum\nolimits_n \tag{9}$$

DOI: 10.13009/EUCASS2023-853

2. β-step: Solve for $s_1, s_2, ..., s_n$ and $\beta_1^*, \beta_2^*, ..., \beta_n^*$ for a given V, p_i and using obtained γ^* from γ-step:

$$[\beta_1^*, \beta_2^*, ..., \beta_n^*] = \max_{\mathbf{s_1, s_2, ..., s_n} \in \sum_\mathbf{n}} \beta_1, \beta_2 ..., \beta_n \quad \text{s.t. :}$$

$$-(V - \gamma^*) + (p_1 - \beta_1)s_1 \in \sum\nolimits_n \tag{10a}$$

$$-(V - \gamma^*) + (p_2 - \beta_2)s_2 \in \sum\nolimits_n \tag{10b}$$

$$\vdots$$

$$-(V - \gamma^*) + (p_n - \beta_n)s_n \in \sum\nolimits_n \tag{10n}$$

3. V-step: Using the obtained γ^*,s_0, $s_1, s_2, ..., s_n$ and $\beta_1^*, \beta_2^*, ..., \beta_n^*$ from previous two steps, solve for a new V which satisfies the following :

$$V - l_1 \in \sum\nolimits_n \tag{11a}$$

$$-\Big[\frac{\partial V}{\partial x} f(x) + l_2\Big] + (V - \gamma^*)s_0 \in \sum\nolimits_n \tag{11b}$$

$$-(V - \gamma^*) + (p_1 - \beta_1^*)s_1 \in \sum\nolimits_n \tag{11c}$$

$$-(V - \gamma^*) + (p_2 - \beta_2^*)s_2 \in \sum\nolimits_n \tag{11d}$$

$$\vdots$$

$$-(V - \gamma^*) + (p_n - \beta_n^*)s_n \in \sum\nolimits_n \tag{11n}$$

4. Scale V: Replace V with V/γ^* after each V-step. This scaling process roughly normalizes V and tends to keep the γ^* computed in the next step (γ-step) close to unity.

5. Repeat all the steps from $1 - 4$ using the scaled V from step 4 to the γ-step as an input. Continue the process until the final feasible LF V is obtained.

Stopping Criteria of the Algorithm: The algorithm can be stopped in the following ways,

A. Numerical Infeasibility:- This criterion stops the algorithm by indicating that it is not possible to obtain any new LF that satisfies all the constraints of step 3 (V-step).

B. Negligently Increment of β:- This condition in the program terminates the algorithm if any two consecutive estimations of all β_i are less than a pre-defined tolerance value. This criteria can be used if the SF is fixed.

C. Fixed Iteration Number:- The algorithm comes to an end after running through all the specified iteration numbers.

The algorithm may also stop for other reasons, like if it does not get the value of any β_i and related s_i in the β-step. This problem can be solved by changing the SF or placing the center of the SF in a new location.

Some discussions about the V-s algorithm are as follows:

Remark 1. In order to implement the $V - s$ algorithm during the γ-step, an initial LF, denoted as V_0, is necessary. Various techniques can be employed to obtain V_0, such as the Lyapunov Equation (LE) based on linearized dynamics (LD) of the system, [Biswas,[23] Li[26]]. According to the proposal by Li,[26] conducting multiple iterations can improve the estimation of the ROA. Upon completion of the algorithm, a final LF V_{1R} and increased β values for all SFs are obtained. However, even with the use of multiple SFs, V_{1R} may not fully encompass the entire potential ROA. To expand the coverage, the algorithm is restarted with V_{1R} as the initial LF for the subsequent iteration round, potentially resulting in an enlarged ROA. Different types of SFs may be employed in each round, and employing different types can sometimes yield better outcomes. However, it is important to note that the LF may become saturated after a certain number of iteration rounds, reaching its maximum coverage and unable to capture additional areas, even with additional rounds. Furthermore, there may be situations where no new LF satisfying constraint (11) can be found, despite the existence of a substantial stable region outside the already captured region of V.

Remark 2. The following degrees are required to satisfy for a feasible solution of (9)-(11), (Wloszek,[16] Biswas,[23] Li[26]),

$$\deg(V) \geq \deg(l_1)$$

$$\deg(p_i) + \deg(s_i) \geq \deg(V), \quad [i = 1, ..., n]$$

$$\deg(V) + \deg(s_0) \geq \max\{\deg(\frac{\partial V}{\partial x} f),\ \deg(l_2)\}$$

DOI: 10.13009/EUCASS2023-853

5. Selection of Shape Function

The utilization of the Shape Function (SF) plays a vital role in obtaining an improved estimation of the region of attraction (ROA). The overall duration of the iteration process is also influenced by the choice of SF. Various types of SFs will yield distinct LFs with different ROAs and total computational times. As per the definition, any positive definite function can be employed as an SF. The below SF with a shifting center x^* is proposed in Li,[26]

$$p(x) = (x - x^*)^T N(x - x^*) \tag{12}$$

The shape matrix N, being a positive definite matrix, plays a significant role in shaping the SF, determining the ROA size, and calculating V. It should be noted that relying on a single fixed value for N might not yield optimal outcomes. As a result, during each iteration round, it is recommended to test various N values and compare the estimated ROA to select the most suitable one. To obtain the SF's shifting center, x^*, we employ a technique introduced in Li.[26] This approach implies that x^* can be calculated by solving the equation of a straight line that passes through the center and intersect the bounded LF. We have given the mathematical expression to choose the shifting center for the 2-D case only. However, the method can be applied for 3-D case also. Let us consider the equations of bounded LF and 2-D straight line are,

$$V(x_1, x_2) = \gamma^* \quad (13a) \qquad x_2 = \tan\theta_1 x_1 \quad (13b)$$

Here, θ_1 is the pre-defined inclination angle of the line, and for every shifting center, there is a fixed θ_1. Consider the solution point or intersection point of the above equations to be (x^*_{1I}, x^*_{2I}). The distance from the center to the point (x^*_{1I}, x^*_{2I}) is given by $\rho_\alpha = \sqrt{x^*_{1I} + x^*_{2I}}$. So, the shifting center is,

$$x_1^* = \sigma\rho_\alpha \cos\theta_1 \quad (14a) \qquad x_2^* = \sigma\rho_\alpha \sin\theta_1 \quad (14b)$$

Where, $\sigma \in (0, 1)$. More discussion about the selection of the value of σ can be found on Biswas[23] and Li.[26] For the 3-D case, we need to consider the following equation for the straight line,

$$x_1 = r\cos\theta_1 \cos\psi_1 \quad (15a) \qquad x_2 = r\cos\theta_1 \sin\psi_1 \quad (15b) \qquad x_3 = r\sin\theta_1 \quad (15c)$$

Here, θ_1 and ψ_1 are the pre-defined elevation and azimuth angles of the line. We can obtain the shifting center (x_1^*, x_2^*, x_3^*) for the 3-D case using the same procedure as in the 2-D case.

6. Simulation Results

Extensive simulations are performed to assess the effectiveness of the suggested approach on the closed-loop dynamics of the Vought F-8 Crusader aircraft, represented by Eq. (1), using the SOSOPT Toolbox.[11] In order to conduct these simulations, an initial LF is required. It is important to note that a new initial LF is needed for each iteration round. In the first round of iteration, the LF is obtained by solving the Lyapunov equation for the linearized dynamics (LD). For subsequent rounds, the LF estimated from the previous round is used as the initial LF for the new round. Moreover, we selected $deg(V) \to [min(2), max(6)]$, $deg(s_0) \to [min(2), max(4)]$, $deg(s_{1,\dots,n}) \to [min(0), max(4)]$, $l_1 = l_2 = 10^{-6}(x'x)$ and $\sigma = 0.8$ to start the simulation. The simulation is terminated by simultaneously employing the stopping criteria A and B.

The selection of the SF and its center, denoted as x^* in Eq. (14), is essential for initiating the simulation in each new iteration round due to their dynamic nature. In the chosen system dynamics described by Eq. (1), which consists of three states, a 3D SF is required. The calculation of the shifted SF's center involves utilizing the 3D linear equation presented in Eq. (15). This equation emphasizes the need for determining the azimuth angle ψ and the elevation angle θ for center calculation. To derive these angles, we consider a unit cuboid with its center located at the system's equilibrium point $(0, 0, 0)$. From the center of the cuboid, lines are drawn to the vertices and midpoints of each surface. By considering the known edge lengths (1 unit in all directions) of the cuboid, we can calculate the azimuth and elevation angles for these vertices and midpoints. The cuboid comprises eight vertices and six surfaces, resulting in a total of 14 angles. The ellipsoidal SF and the corresponding angles (given in degrees) are provided below.

$$p = \begin{bmatrix} x_1 - x_1^* \\ x_2 - x_2^* \\ x_3 - x_3^* \end{bmatrix} N \begin{bmatrix} x_1 - x_1^* \\ x_2 - x_2^* \\ x_3 - x_3^* \end{bmatrix}; \quad N = \begin{bmatrix} 1 & 0 & 0 \\ 0 & 0.5 & 0 \\ 0 & 0 & 0.5 \end{bmatrix} \tag{16}$$

DOI: 10.13009/EUCASS2023-853

$$\begin{bmatrix} \psi \\ \theta \end{bmatrix} = \begin{bmatrix} -45 & -45 & -135 & -135 & 45 & 45 & 135 & 135 & 0 & 90 & 180 & -90 & 0 & 0 \\ -35 & 35 & -35 & 35 & -35 & 35 & -35 & 35 & 0 & 0 & 0 & 0 & 90 & -90 \end{bmatrix} \tag{17}$$

The primary eight angles correspond to the vertices of the unit cuboid, while the last six angles correspond to the middle points of its surfaces. In order to demonstrate the simulation results, we conducted three rounds of iteration. In the first round, a single ellipsoid centered at the origin ($x_1^* = x_2^* = x_3^* = 0$) was utilized, with a shape matrix given by Eq. (16). During the second and third rounds of the simulation, we utilized a total of 16 SFs, all of which are identical to the SF described in Eq. (16). Additionally, we calculated the centers of these SFs using the corresponding angles outlined in Eq. (17).

The results presented in Fig. 1(a), Fig. 1(b), and Fig. 1(c) demonstrate the growth of estimated ROA from the initial round to the subsequent round. This growth is attributed to the utilization of multiple SFs in different locations. With each iteration, these SFs expand, and the algorithm generates a new Lf to encompass all the enlarged SFs. This process continues until the algorithm becomes infeasible. To maintain the visibility of the SFs, only the final results from each round are shown in the figures. Fig. 1(d) compares the estimated ROAs from all rounds with the result obtained from the linearized dynamics. Moreover, Fig. 1(e), Fig. 1(f), and Fig. 1(g) illustrate the projection of the estimation on the $\alpha - \theta$, $\alpha - q$, and $\theta - q$ planes at $q = 0$, $\theta = 0$, and $\alpha = 0$, respectively.

The paper by Zhao[24] designed a controller with ROA estimation based on a single SF in the sum-of-squares optimization method. They presented a projection of the ROA estimation on the $\alpha - \theta$ plane at $q = 0$. In our study, we utilized their controller in a closed-loop system and estimated the ROA using multiple SFs. The comparison of the ROA estimated with multiple SFs and the result presented in Zhao[24] is shown in Fig.1(h), demonstrating that the designed controller has a larger ROA than previously reported.

Additionally, Fig. 1(i) presents a plot of the responses of the closed-loop F-8 aircraft dynamics with a total of 12 initial conditions, including 8 inside and 4 outside of the estimated ROA. The inside initial conditions are $\alpha(0) = [-0.5; -0.5; 0.5; 0.5; 0.1; -0.1; 0.7; -0.7]$, $\theta(0) = [2; -3; 2, -3; 2.9; -3.5; 0.1; -0.1]$, and $q(0) = [5; -3; 2.8; -5.5; 1.8; -3; 3; -3]$, while the outside initial conditions are $\alpha(0) = [-0.1; -0.9; 0.9; 0.1]$, $\theta(0) = [-5; -1; 1; 5]$, and $q(0) = [-7; -7; 6; 6]$. It is evident that the trajectories converge to the EP/origin for all the inside initial conditions, indicating that the obtained ROA provides a safe and stable operating region. However, the first of the outside initial conditions yields a stable trajectory, while the other three results in unstable trajectories, suggesting the presence of a stable region outside the estimated ROA. The estimation process was terminated after the third round, but it can be further continued to achieve even larger ROA estimations. Notably, the existing methods [Wloszek,[16] Chakraborty,[20] Khrabrov[21]] that rely on a single SF produce similar results to those obtained from the first round, where only one SF was used. A comparison of the results depicted in Fig. 1(d) reveals that the suggested approach offers superior outcomes. The entire simulation process lasted 6004 seconds, encompassing 123, 28, and 32 iterations in the first, second, and third rounds, respectively.

7. Conclusion

This paper demonstrated the effectiveness of employing multiple Shape Functions (SFs) within the SOS optimization framework. Extensive simulations were conducted on the closed-loop polynomial dynamics of the Vought F-8 Crusader aircraft, highlighting the applicability of this approach in analyzing the ROA for the aircraft's flight control system. One notable advantage of this technique is its capability to estimate a larger ROA, thereby providing an expanded safe and stable operating region for the controller. However, it is important to acknowledge certain limitations of the current method. The outcomes are influenced by factors such as the type (N) and quantity of SFs utilized, as well as the selection of SF centers, which can significantly impact the results. In this study, the SFs and their corresponding angles for center positioning were manually chosen. Adopting a more structured approach in selecting these components has the potential to enhance the obtained results.

Acknowledgments

The first author acknowledges the Government of India, Ministry of Social Justice and Empowerment for supporting the studies under the National Overseas Scholarship for Ph.D. with scholarship number 11015/33/2019 SCD-V NOS.

DOI: 10.13009/EUCASS2023-853

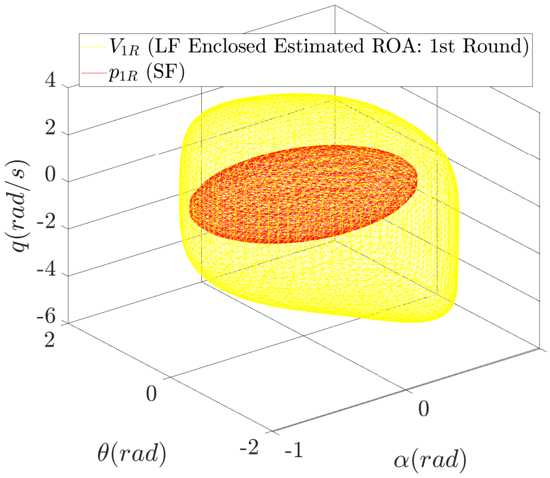

(a) Estimated ROA from 1st Round

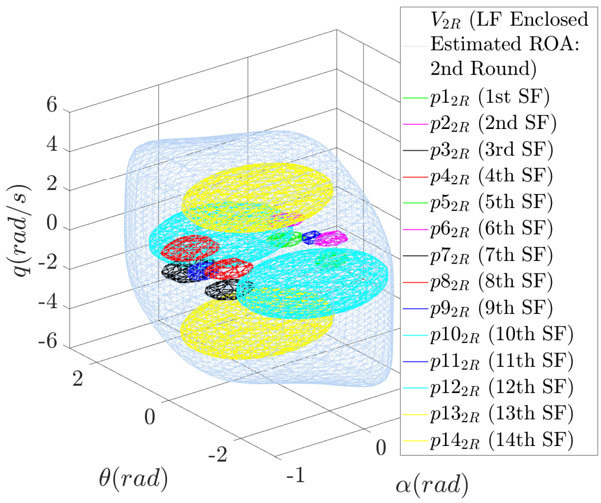

(b) Estimated ROA from 2nd Round

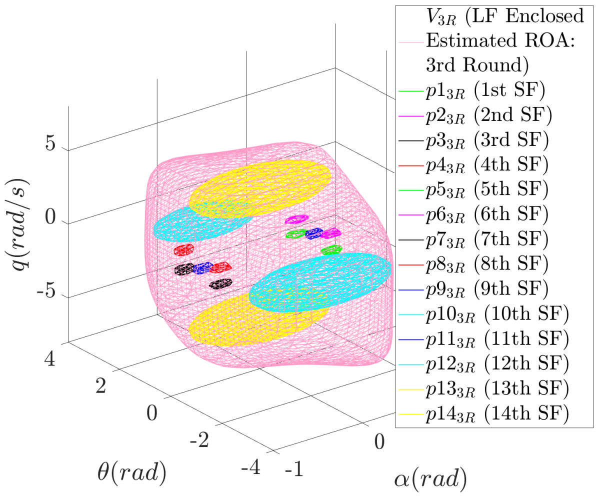

(c) Estimated ROA from 3rd Round

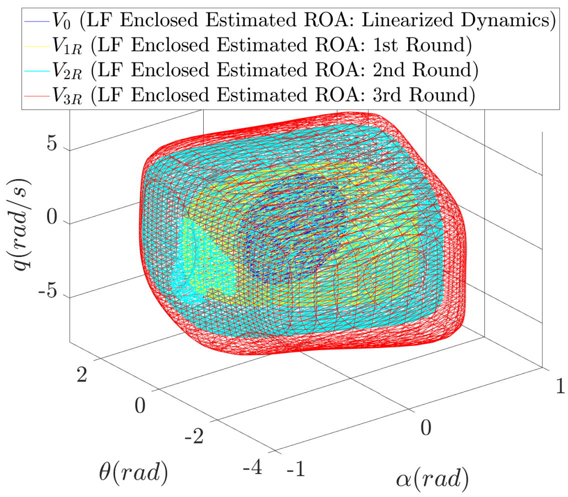

(d) Comparison Among Results from all the Rounds

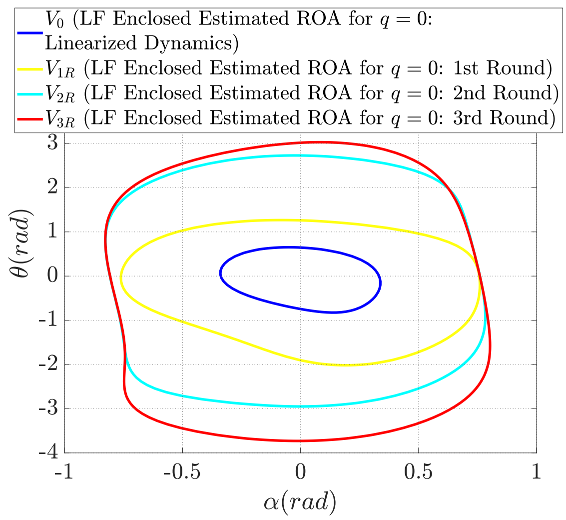

(e) Cross Section of Estimated ROA for $q = 0$

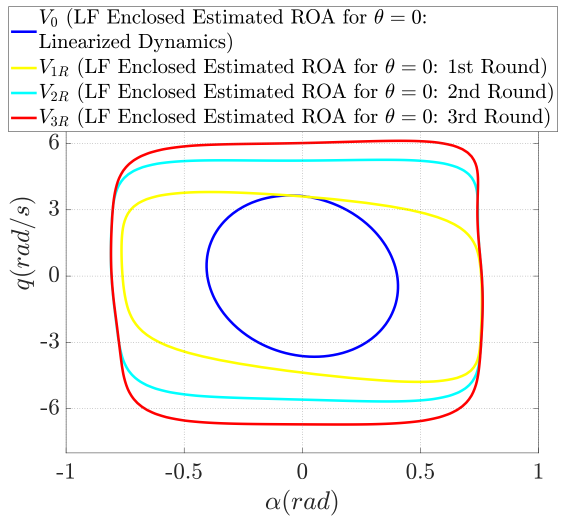

(f) Cross Section of Estimated ROA for $\theta = 0$

DOI: 10.13009/EUCASS2023-853

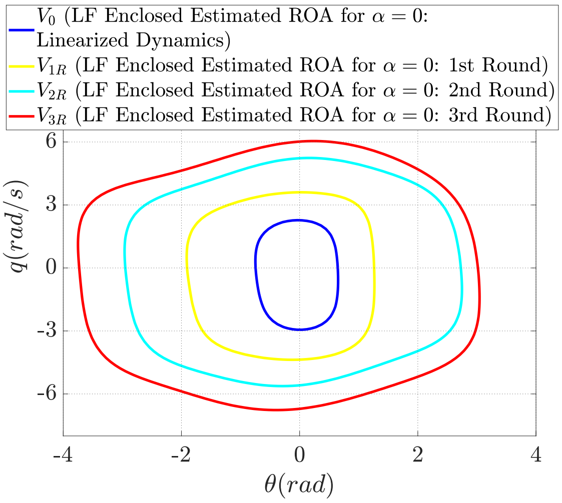

(g) Cross Section of Estimated ROA for $\alpha = 0$

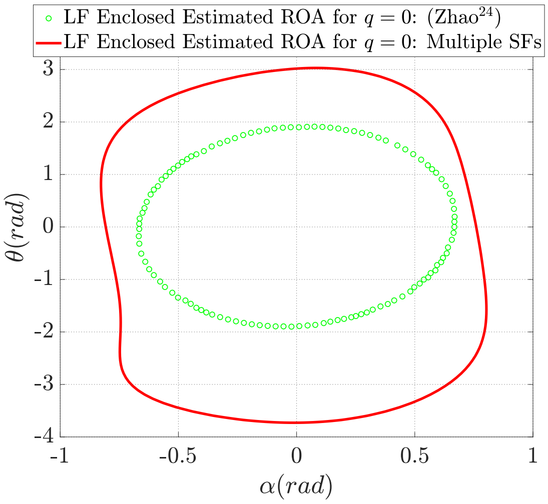

(h) Cross-Sectional Comparison of the Estimated ROA for $q = 0$

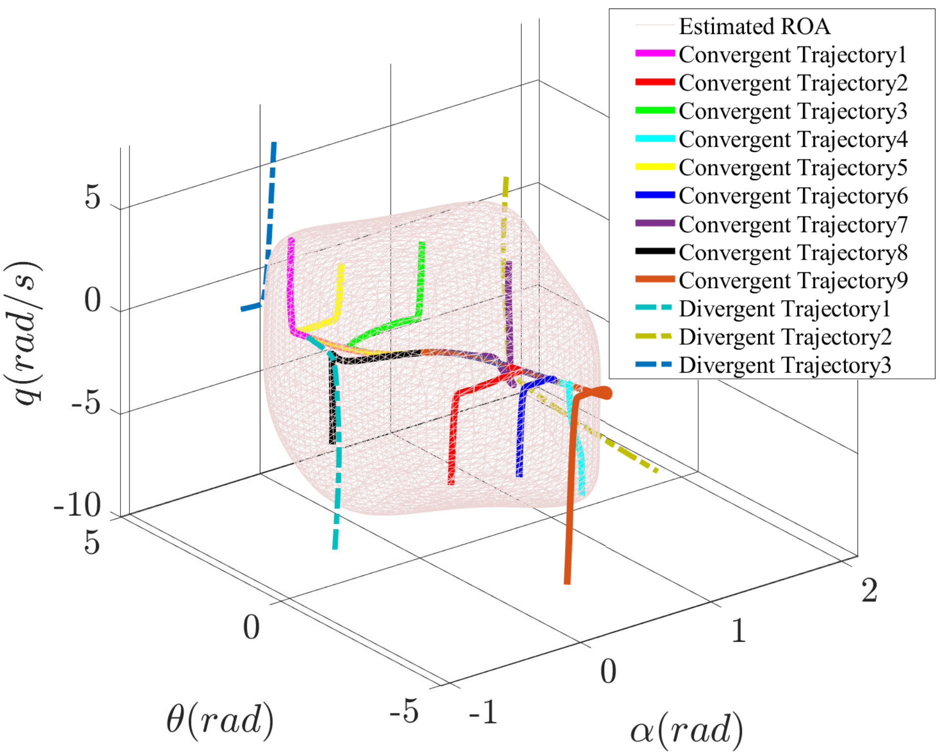

(i) Estimated ROA and Trajectories of the Closed-loop System

Figure 1: Estimated ROA Using Multiple Shape Functiions

DOI: 10.13009/EUCASS2023-853

References

[1] Khalil, K. H. (2002). *Nonlinear Systems*. 3rd Edition, Prentice Hall, Inc.

[2] VanAntwerp, J. G. and Braatz, R. D., "A Tutorial on Linear and Bilinear Matrix Inequalities," *Journal of Process Control*, Vol. 10, No. 4, pp. 363-385, 2000, https://doi.org/10.1016/S0959-1524(99)00056-6.

[3] Tibken, B., "Estimation of the Domain of Attraction for Polynomial Systems via LMIs," *Proceedings of the 39th IEEE Conference on Decision and Control*, vol.4, pp. 3860-3864, 2000, doi: 10.1109/CDC.2000.912314.

[4] Powers, V. and Wormann, T., "An Algorithm for Sums of Squares of Real Polynomials," *Journal of Pure and Applied Algebra*, Vol. 127, No. 1, pp. 99-104, 2000, https://doi.org/10.1016/S0022-4049(97)83827-3.

[5] Parrilo, P. A., *Structured Semidefinite Programs and Semi-algebraic Geometry Methods in Robustness and Optimization,* Ph.D. Thesis, California Institute of Technology, 2000, doi.10.7907/2K6Y-CH43.

[6] Parrilo, P. A., "Semidefinite Programming Relaxations for Semi-Algebraic Problems," *Mathematical Programming*, 96(2):293â320, 2003, https://doi.org/10.1007/s10107-003-0387-5.

[7] Balas, G.; Packard, A.; Seiler, P. and Topcu, U., *Robustness Analysis of Nonlinear Systems*, 2009, http://users.cms.caltech.edu/˜utopcu/saveMaterial/LangleyWorkshop.html

[8] Peet, M. M., *LMI Methods in Optimal and Robust Control*, 2020, http://control.asu.edu/MAE598_frame.htm.

[9] Papachristodoulou, A. and Prajna, S., "A Tutorial on Sum of Squares Techniques for Systems Analysis," *Proceedings of the 2005, American Control Conference*, Vol. 4, pp. 2686-2700, 2005, doi: 10.1109/ACC.2005.1470374.

[10] Cunis, T.; Legat, B., "Sequential Sum-of-Squares Programming for Analysis of Nonlinear Systems," *ArXivorg*, 2022, https://doi.org/10.48550/arXiv.2210.02142.

[11] Seiler, P., "SOSOPT: A Toolbox for Polynomial Optimization," 2016, https://doi.org/10.48550/arXiv.1308.1889.

[12] Papachristodoulou, A.; Anderson, J.; Valmorbida, G.; Prajna, S.; Seiler, P.; Parrilo, P.; Peet, M. M. and Jagt, D., "SOSTOOLS Version 4.00 Sum of Squares Optimization Toolbox for MATLAB," *ArXivorg*, 2013, https://doi.org/10.48550/arXiv.1310.4716.

[13] Ahmadi, A. A., *Sum of Squares (SOS) Techniques : An Introduction*, 2016, https://www.princeton.edu /~aaa/Public/Teaching/ORF523/ORF523_Lec15.pdf.

[14] Lall, S., *Sums of Squares*, 2011, https://web.stanford.edu/class/ee364b/lectures/sos_slides.pdf.

[15] Kunisky, D., *Lecture Notes on Sum-of-Squares Optimization*, 2022, http://www.kunisky.com/static/teaching /2022spring-sos/sos-notes.pdf.

[16] Wloszek, Z. J.; Feeley, R.; Weehong, T.; Sun, K. and Packard, A., "Control Applications of Sum of Squares Programming," *Lecture Notes in Control and Information Sciences*, Vol. 312, pp. 580-508, 2005, https://doi.org/10.1007/10997703_1.

[17] Tan, W.; and Packard, A., "Searching for Control Lyapunov Functions Using Sums of Squares Programming," *42nd Annual Allerton Conference on Communications, Control and Computing*, pp. 210-219, 2004.

[18] Jarvis-Wloszek, Z., *Lyapunov Based Analysis and Controller Synthesis for Polynomial Systems using Sum-of-Squares Optimization*, PhD thesis, University of California, Berkeley, 2003.

[19] Tan, W., *Nonlinear Control Analysis and Synthesis using Sum-of-Squares Programming*, PhD thesis, University of California, Berkeley, 2006.

[20] Chakraborty, A.; Seilera, P. and Balasa, G., "Nonlinear Region of Attraction Analysis for Flight Control Verification and Validation," *Control Engineering Practice*, Vol. 19, No. 4, pp. 335-345, 2011, https://doi.org/10.1016/j.conengprac.2010.12.001.

[21] Khrabrov, A.; Sidoryuk, M. and Ignatyev, D., "Estimation of Regions of Attraction of Spin Modes," *7th European Conference for Aerospace Sciences*, 2017, https://doi: 10.13009/EUCASS2017-312.

DOI: 10.13009/EUCASS2023-853

[22] Li, D.; Tsourdos, A.; Wang, Z. and Ignatyev, D., "Nonlinear Analysis for Wing-Rock System with Adaptive Control," *Journal of Guidance, Control, and Dynamics*, Vol. 45, No. 11, pp. 2174-2181, 2022, https://doi.org/10.2514/1.G006775.

[23] Biswas, B.; Ignatyev, D.; Zolotas, A. and Tsourdos, A., "Region of Attraction Estimation Using Union Theorem in Sum-of-Squares Optimization," *ArXivorg*, 2023, https://doi.org/10.48550/arXiv.2305.11655.

[24] Zhao, Z.; Feeley, R.; Wang, J., "Stability Analysis and Design for Polynomial Nonlinear Systems Using SOS with Application to Aircraft Flight Control," *IFAC Proceedings Volumes*, Vol. 41, No. 2, pp. 8684-8689, 2008, https://doi.org/10.3182/20080706-5-KR-1001.01468.

[25] Vidyasagar, M., *Nonlinear Systems Analysis*, 2nd Edition, Prentice Hall, Inc., 1993.

[26] Li, D.; Ignatyev, D.; Tsourdos, A. and Wang, Z., "Estimation of Non-Symmetric and Unbounded Region of Attraction using Shifted Shape Function and R-composition," *ISA Transactions*, 2022, https://doi.org/10.1016/j.isatra.2022.11.015.